PASJ: Publ. Astron. Soc. Japan **59**, 827–834, 2007 August 25

A New Model for the Structure of the DACs and SACs Regions in the Oe and Be Stellar Atmospheres

Emmanouel DANEZIS,[1] Dimitris NIKOLAIDIS,[1] Evaggelia LYRATZI,[1] Luka Č. POPOVIĆ,[2]
Milan S. DIMITRIJEVIĆ,[2] Antonis ANTONIOU,[1] and Efstratios THEODOSIOU[1]
[1]*University of Athens, Faculty of Physics, Department of Astrophysics, Astronomy and Mechanics, Panepistimioupoli, Zographou 157 84, Athens, Greece*
[2]*Astronomical Observatory of Belgrade, Volgina 7, 11160 Belgrade, Serbia, Isaac Newton Institute of Chile, Yugoslavia Branch*
edanezis@phys.uoa.gr, dlnrrr@tellas.gr, elyratzi@phys.uoa.gr, lpopovic@aob.bg.ac.yu, mdimitrijevic@aob.bg.ac.yu, ananton@phys.uoa.gr, etheodos@phys.uoa.gr

(Received 2007 March 14; accepted 2007 May 1)

Abstract

We present a new mathematical model for the density regions where a specific spectral line and its SACs/DACs are created in the Oe and Be stellar atmospheres. In calculations of final spectral line function we consider that the main processes for the line broadening are the rotation of the density regions creating the spectral line and its DACs/SACs, as well as the random motions of the ions. This line function is able to reproduce the spectral feature, which enables us to calculate some important physical parameters, such as the rotational, radial, and random velocities, the full width at half maximum, the Gaussian deviation, the optical depth, the column density, and the absorbed or emitted energy. Additionally, we can calculate the percentage of the contribution of the rotational velocity and the ions' random motions of the DACs/SACs regions to the line broadening. Finally, we present two tests and three short applications of the proposed model.

Key words: stars: early type, emission-line — ultraviolet: stars

1. Introduction

When we study the UV lines of hot emission stars we have to deal with two problems: (i) The presence of a very complex structure of many spectral lines in the UV region, such as the resonance lines of Si IV, C IV, N V, Mg II, and the N IV spectral line. (ii) The presence of Discrete Absorption Components (DACs, Bates & Halliwell 1986).

DACs are discrete, but not unknown, absorption spectral lines. They are spectral lines of the same ion and the same wavelength as a main spectral line, shifted at different $\Delta\lambda$, since they are created in different density regions, which rotate and move radially with different velocities (Danezis 1983, 1987; Danezis et al. 2003; Lyratzi et al. 2007). DACs are lines, easily observed in the case that the regions that give rise to them rotate with low velocities and move radially with high velocities.

Many suggestions have been made to explain the DACs phenomenon. Most researchers have suggested mechanisms that allow the existence of structures which cover all or a significant part of the stellar disk, such as shells, blobs, or puffs (Underhill 1975; Henrichs 1984; Underhill & Fahey 1984; Bates & Halliwell 1986; Grady et al. 1987; Lamers et al. 1988; Waldron et al. 1992, 1994; Cranmer & Owocki 1996; Rivinius et al. 1997; Kaper et al. 1996, 1997, 1999; Markova 2000). Some researchers have also suggested interaction of fast and slow wind components, Corotation Interaction Regions (CIRs), and structures due to magnetic fields or spiral streams as a result of the stellar rotation (Underhill & Fahey 1984; Mullan 1984a, 1984b, 1986; Prinja & Howarth 1988; Cranmer & Owocki 1996; Fullerton et al. 1997; Kaper et al. 1996, 1997, 1999; Cranmer et al. 2000). Though we do not yet know the mechanism responsible for the formation of such structures, it is positive that DACs result from independent high-density regions in the stellar environment.

An important question is whether there is a connection between the observed complex structure of the above-mentioned spectral lines and the presence of DACs. A possible answer is that if the regions that create the DACs rotate with large velocities and move radially with small velocities, the produced lines would have large widths and small shifts. As a result, they are blended among themselves as well as with the main spectral line, and thus they are not discrete. In such a case the name Discrete Absorption Components is inappropriate, and we use only the name Satellite Absorption Components (SACs) (Lyratzi & Danezis 2004; Danezis et al. 2005, 2006; Nikolaidis et al. 2006; D. Nikolaidis et al. 2006, presentation in 26th IAU General Assembly). A very important question is whether it is possible that the existence of SACs may be responsible for the complex structure of the observed spectral feature.

As is clear, for a future study of the mechanisms responsible for the creation of density regions that produce the complex profiles of the above-mentioned spectral lines, as well as for a study of their structure and evolution, we need to calculate the values of some physical parameters of these regions.

In order to calculate these parameters, it is necessary to construct a line function, based on the idea of DACs

and SACs phenomena able to reproduce, in the best way, the observed spectral feature.

Danezis et al. (2003) presented such a line function in the case that the process of the line broadening is only the rotation of the regions that create the observed spectral lines and their components and when these regions present spherical symmetry around their own center or the center of the star (see also Lyratzi et al. 2007). With this line function we can calculate some important physical parameters, such as the rotational and the radial velocities, the optical depth, the column density (Danezis et al. 2005) and the absorbed/emitted energy. However, in some cases the chaotic motion of emitters/absorbers inside the dense layers can be significant (see e.g., Danezis et al. 2006) and the estimated rotation might be overestimated. Therefore, a modification of the previously given model (Danezis et al. 2003) is needed, in sense that the possible contribution of random velocities to the line broadening can be taken into account.

Here, we present a new model that also includes the random motions of the ions, since in the case of hot emission stars one can expect a significant contribution of random motion of the emitters/absorbers to the line profile. Based on this idea, besides the above-mentioned physical parameters of the regions that create the complex spectral lines, we can calculate the mean random velocity of the ions, but also the percentage of the contribution of the rotational velocity and emitter/absorber random motions of the DACs/SACs regions to the line broadening, as well as the Gaussian deviation for each DAC/SAC profile.

This paper is organized as follows: In section 2 we give a description of the model. In section 3 we discuss it, in section 4 we give two tests, and in section 5 we present applications. Finally, in section 6 we outline our conclusions.

2. Description of the Model — the Line Function

As was already mentioned above, Danezis et al. (2003) presented a line function that is able to accurately reproduce the observed spectral lines and their SACs/DACs at the same time. The proposed line function is

$$F_{\lambda\mathrm{final}} = \left[F_0(\lambda) \prod_i e^{-L_i \xi_i} + \sum_j S_{\lambda \mathrm{e}j} \left(1 - e^{-L_{\mathrm{e}j} \xi_{\mathrm{e}j}}\right) \right] e^{-L_g \xi_g}, \tag{1}$$

where: $F_0(\lambda)$ is the initial radiation flux; L_i, $L_{\mathrm{e}j}$, and L_g are the distribution functions of the absorption coefficients ($k_{\lambda i}$, $k_{\lambda \mathrm{e}j}$, and $k_{\lambda g}$, respectively). Each L depends on the values of the apparent rotational velocity as well as of the radial velocity of the density shell, which forms the spectral line (V_{rot}, V_{rad}); ξ_i is the optical depth in the center of the line; $S_{\lambda \mathrm{e}j}$ is the source function, which, at the moment when the spectrum is taken, is constant.

In equation (1), the functions $e^{-L_i \xi_i}$, $S_{\lambda \mathrm{e}j} \left(1 - e^{-L_{\mathrm{e}j} \xi_{\mathrm{e}j}}\right)$, $e^{-L_g \xi_g}$ are the distribution functions of each satellite component; we can replace them with a known distribution function (Gauss, Lorentz, Voigt, or disk model). An important fact is that in the calculation of $F(\lambda)$ we can include different geometries (in the calculation of L) of the absorbing or emitting independent density layers of matter.

A decision concerning the geometry is essential to calculate the distribution function that we use for each component; i.e. for different geometries we have different line shapes, representing the considered SACs.

Equation (1) gives a function of the complex profile of a spectral line, which presents SACs or DACs. This means that equation (1) is able to reproduce not only the main spectral line, but its SACs as well.

The main hypotheses when we constructed the rotation distribution function were that the line width, $\Delta\lambda$, is only due to rotation of the regions that create the observed spectral lines and their components, and that these regions present spherical symmetry around their own center, or the center of the star (see also Lyratzi et al. 2007). Consequently, the random velocities of the emitters/absorbers in the density region are assumed to be negligible, i.e., they do not significantly contribute to the line profile. Here, we consider that the random velocities may have a significant contribution to the distribution function, L (see Appendix). In this case the final form of L is given as

$$L(\lambda) = \frac{\sqrt{\pi}}{2\lambda_0 z} \int_{-\frac{\pi}{2}}^{\frac{\pi}{2}} \left[\mathrm{erf}\left(\frac{\lambda - \lambda_0}{\sigma\sqrt{2}} + \frac{\lambda_0 z}{\sigma\sqrt{2}} \cos\theta \right) - \mathrm{erf}\left(\frac{\lambda - \lambda_0}{\sigma\sqrt{2}} - \frac{\lambda_0 z}{\sigma\sqrt{2}} \cos\theta \right) \right] \cos\theta \, d\theta, \tag{2}$$

where λ_0 is the transition wavelength of a spectral line that arises from a specific point of the equator of a spherical density region that produces one satellite component, $z = \dfrac{V_{\mathrm{rot}}}{c}$ (V_{rot} is the rotational velocity of the specific point) and $\mathrm{erf}(x) = \dfrac{2}{\pi} \displaystyle\int_0^x e^{-u^2} du$ is the function that describes the Gaussian error distribution.

3. Discussion and Way of Application of the Proposed Model

Introducing the previous final function of a complex spectral line [equation (1)], in combination with the distribution function, L, given in equation (2), we note the following:

1. The proposed line function [equation (1)] can be used for any number of absorbing or emitting regions. This means that it can also be used in the simple case that $i = 1$ and $j = 0$ or $i = 0$ and $j = 1$, meaning when we deal with simple, classical absorption or emission spectral lines, respectively. This allows us to calculate all of the important physical parameters, such as the rotational, radial, and random velocities, the full width at half maximum, the Gaussian deviation, the optical depth, the column density (Danezis et al. 2005), and the absorbed or emitted energy, for all simple and classical spectral lines in all spectral ranges.

2. For each group of parameters (V_{rot_i}, V_{rad_i}, V_{rand_i}, and ξ_i), the function $I_{\lambda i} = e^{-L_i \xi_i}$ reproduces the spectral line profile formed by the i density region of matter, meaning that for each group we have a totally different profile. This results

in the existence of only one group of V_{rot_i}, V_{rad_i}, V_{rand_i}, and ξ_i giving the best fit of the i component. In order to accept that as the best fit of the observed spectral line, given by the groups (V_{rot_i}, V_{rad_i}, V_{rand_i}, ξ_i) of all calculated SACs, one has to adhere to all physical criteria and techniques, such as:

i) To make a complete identification of spectral lines in the region around the studied spectral line and to have the superposition of the spectral region that we study with the same region of a classical star of the same spectral type and luminosity class, in order to identify the existence of spectral lines that blend with the studied ones, as well as the existence of SACs.

ii) The resonance lines as well as all lines originating in a particular region should have the same number of SACs, depending on the structure of this region, without any influence of the ionization stage or ionization potential of the emitters/absorbers. As a consequence, the respective SACs should have similar values of the radial and rotational velocities.

iii) The ratio of the optical depths of two resonance lines must be the same as the ratio of the respective relative intensities.

3. In order to decide which group of parameters gives the best fit, we propose a model according to the following two steps:

(i) In the first step we consider that the main process for line broadening of the main line and satellite components is rotation of the region that creates the components of the observed feature; a secondary cause is thermal Doppler broadening. This means that we start fitting the line using the maximum V_{rot}. We then include Doppler broadening, in order to accomplish the best fit (rotation case). (ii) In the second step, we consider the opposite. In this case the main process of line broadening of the main line and satellite components is supposed to be Doppler broadening; a secondary process is rotation of the regions that create the components of the observed feature. This means that we start fitting the line using the maximal Doppler broadening. We then include V_{rot}, in order to accomplish the best fit (Doppler case).

In both cases (rotation case and Doppler case) we check the correct number of satellite components that construct the whole line profile. At first we fit using the number of components that give the best difference graph between the fit and the real spectral line. We then make a fit using one component less than in the previous fit. The F-test between them allows us to take the correct number of satellite components that construct in the best way the whole line profile. The F-test between these two cases indicates the best way to fit spectral lines. When the F-test cannot give a definite conclusion on which case we should use, we can still obtain information about the limits of V_{rot} and σ. If the F-test gives similar values, then the rotation case defines the maximal V_{rot} and the minimal σ and the Doppler case defines the minimal V_{rot} and the maximal σ.

4. The profiles of each main spectral line and its SACs are fitted by the function $e^{-L_i \xi_i}$ in the case of an absorption component, or $S_{\lambda \mathrm{e}j}\left(1-e^{-L_{\mathrm{e}j}\xi_{\mathrm{e}j}}\right)$ in the case of an emission component. These functions produce symmetrical line profiles. However, most of the spectral lines are asymmetric. This fact is interpreted as being a systematical variation of the apparent radial velocities of the density regions where the main spectral line and its SACs are created. In order to approximate those asymmetric profiles we have chosen a classical method. This is the separation of the region that produces asymmetric profiles of the spectral line, into a small number of sub-regions, and each of them is treated as an independent absorbing shell. In this way we can study the variation of the density, the radial shift and the apparent rotation as a function of the depth in every region that produces a spectral line with an asymmetric profile. Everything mentioned above must be taken into account during an evaluation of our results; also, one should not consider that the evaluated parameters of those sub-regions correspond to independent regions of matter, which form the main spectral line or its SACs.

5. We suggest that the width of the blue wing is the result of the composition of profiles of the main spectral line and its SACs. Thus, the blue wing of each SAC gives the apparent rotational velocity of the density shell, in which it forms. In order to conduct measurements with physical meaning, we should not calculate the width of the blue wing of the observed spectral feature, but the width of the blue wing of each SAC.

6. We would like to point out that the final criterion to accept or reject a best fit is the ability of the calculated values of the physical parameters to give us a physical description of the events developing in the regions where the spectral lines presenting SACs are created.

7. In the proposed distribution function an important factor is $m = \dfrac{\lambda_0 z}{\sqrt{2}\sigma}$. This factor indicates the kind of the distribution function that is able to fit in the best way each component's profile.

i) If $m \simeq 3$, we have equivalent contributions of the rotational and random motions to the line widths.

ii) If $m \simeq 500$, the line broadening is only an effect of the rotational velocity, and the random velocity is negligible. In this case, the profile of the line is the same as the theoretical profile derived from the rotation distribution function.

iii) Finally, if $m < 1$, the line broadening is only an effect of random velocities and the line distribution is Gaussian.

4. Testing the Model

In order to check the validity of our model we perform two tests:

I) In order to check the above spectral line function, we calculated the rotational velocity of He I λ 4387.928 Å absorption line for five Be stars, using two methods, the classical Fourier analysis and our model. In figure 1 we present five He I λ 4387.928 Å fittings for the studied Be stars and the measured rotational velocities with both methods. The obtained rotational velocities from our model are in good agreement with ones obtained with Fourier analysis.

The values of the rotational velocities, calculated with Fourier analysis, some times, may present small differences compared to those calculated with our method, because in Fourier analysis the total broadening of the spectral lines is assumed to represent the rotational velocity. On the contrary, our model accepts that a part of this broadening arises from the random motion of the ions.

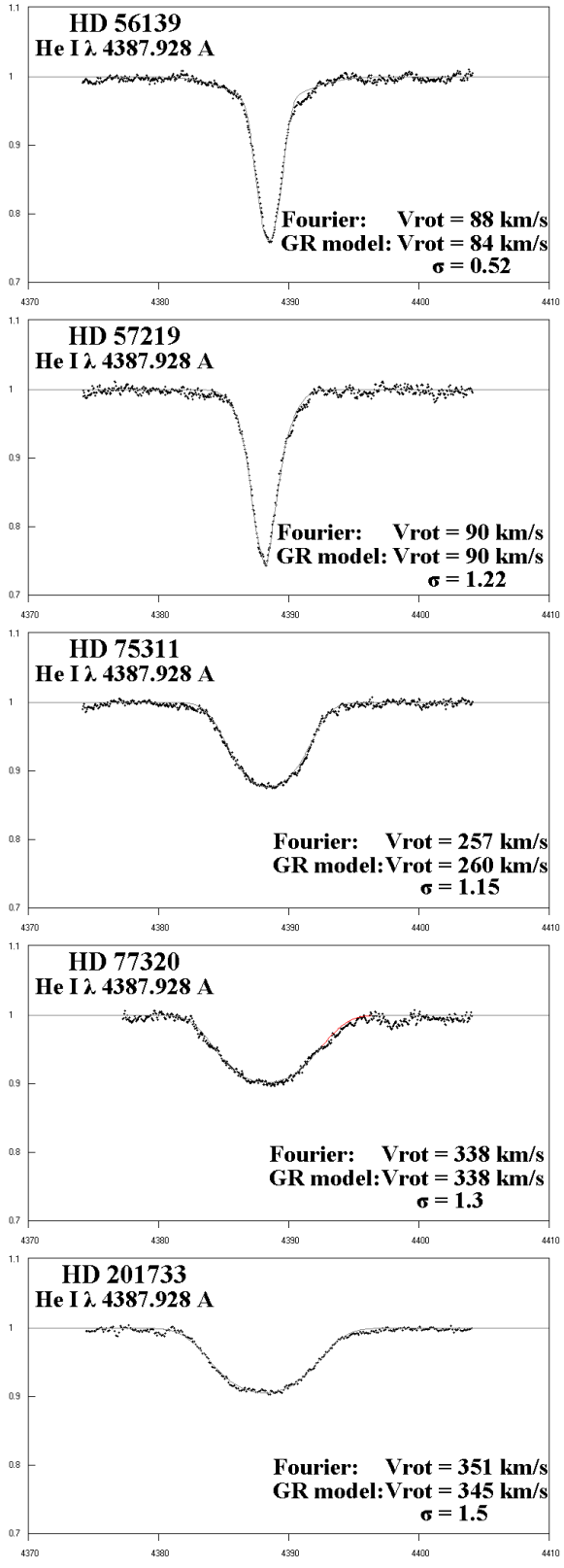

Fig. 1. Five He I λ 4387.928 Å fittings for the studied Be stars with the GR model and the measured rotational velocities with Fourier analysis and the GR model. The differences between the observed and reproduced spectral lines are hard to see, as we have accomplished the best fit.

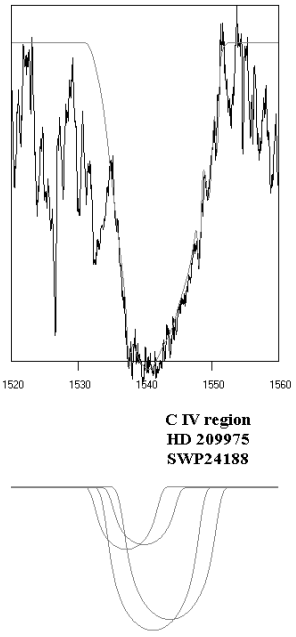

Fig. 2. C IV resonance lines (λλ 1548.155, 1550.774 Å) best fit with the GR model for the star HD 209975. The components obtained from the best fit are shown at the bottom.

We point out that with our model, apart from the rotational velocities, we can also calculate some other parameters, such as the standard Gaussian deviation, σ, the velocity of random motions of emitters/absorbers, the radial velocities of the regions producing studied spectral lines, the full width at half maximum (FWHM), the optical depth, the column density, and the absorbed or emitted energy.

II) An additional test of our model is to calculate the random velocities of layers that produce the C IV satellite components of 20 Oe stars with different rotational velocities.

We analyzed the C IV line profiles of 20 Oe stars, the spectra of which were observed with the IUE - satellite (IUE Archive Search database[1]). We examined the complex structure of the C IV resonance lines (λλ 1548.155, 1550.774 Å). Our sample included the subtypes O4 (one star), O6 (four stars), O7 (five stars), O8 (three stars), and O9 (seven stars). The values of the photospheric rotational velocities were taken from the catalogue of Wilson (1963) (see also Antoniou et al. 2006).

In the composite C IV line profiles we detect two components in 9 stars, three in 7 stars, four in 3 stars, and five in one star.

In figure 2 we present the C IV resonance lines best fit for the star HD 209975.

In figure 3 we present random velocities ($V_{\rm rand}$) of each SAC as a function of the photospheric rotational velocity ($V_{\rm phot}$) for all of the studied stars.

As one can see in figure 3, the obtained values for random velocities are in accordance with classical theory; the values of the random velocities do not depend on the inclination angle

[1] ⟨http://archive.stsci.edu/iue/search.php⟩.

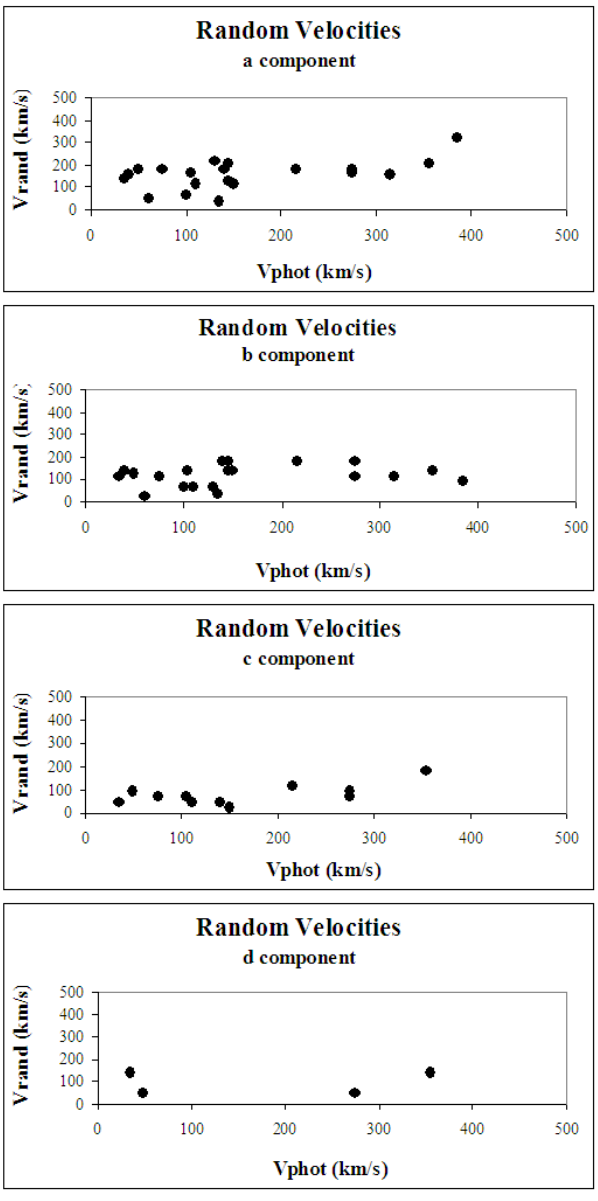

Fig. 3. Random velocities ($V_{\rm rand}$) of the four SACs as a function of the photospheric rotational velocity ($V_{\rm phot}$) for all of the studied Oe stars.

of the rotational axis. Because the ionization potential of the regions where satellite components are created is the same for all studied stars, one can expect similar average values of the random velocities for each absorbing region (here denoted as the a–d components; see figure 3) for all studied stars, as we obtained by using the model.

Both of the tests, described above, support our new approach to investigating the regions around hot stars, implying that besides rotation of the regions, one should also consider the random motion of emitters/absorbers.

5. Applications of the Model: Rotation – Density Regions vs. Photosphere

Here, we give some examples of applications of the model. We apply the model to study the complex structure of C IV and Si IV spectral lines in Oe and Be stars, as well as the rotational velocities of different components, in order to find a more precise rotational component.

5.1. C IV Density Regions of 20 Oe Stars

In this application we use the previously mentioned C IV IUE spectra of the second test. We study the relation between the ratio $V_{\rm rot}/V_{\rm phot}$ of the first, second, third, and fourth detected components with the photospheric rotational velocity ($V_{\rm phot}$). This ratio indicates how much the rotational velocity of the specific C IV layer is higher than the apparent rotational velocity of a star (see also Antoniou et al. 2006). In figure 4 we present our results.

In each region and for each component we can conclude that there exists an exponential relation between the ratio $V_{\rm rot}/V_{\rm phot}$ and the photospheric rotational velocity, $V_{\rm phot}$. The maximum ratio, $V_{\rm rot}/V_{\rm phot}$, varies from 40 for the first to 5 for the fourth component (figure 4). A possible explanation of this situation is the inclination of the stellar axis.

5.2. Si IV Density Regions of 27 Be Stars

This study was based on an analysis of 27 Be stellar spectra taken with the IUE-satellite. We examined the complex structure of the Si IV resonance lines ($\lambda\lambda$ 1393.755, 1402.77 Å). Our sample included all subtypes from B0 to B8. The values of the photospheric rotational velocities were taken from the catalogue of Chauville et al. (2001).

We found that the Si IV spectral lines consist of three components in 7 stars, four in 15 stars, and five in 5 stars. We studied the relation between the ratio $V_{\rm rot}/V_{\rm phot}$ of the first, second, third, fourth, and fifth detected components with the photospheric rotational velocity ($V_{\rm phot}$). This ratio indicates how much the rotational velocity of the specific Si IV layer is higher than the apparent rotational velocity of the star (see also Lyratzi et al. 2006). In figure 5 we present our results.

The Si IV resonance lines are composed of three, four, or five components. The difference from the case of the C IV resonance lines in the spectra of 20 Oe stars is that they are composed of two, three, or four components. However, in both cases, in each region and for each component there exists an exponential relation between the ratio $V_{\rm rot}/V_{\rm phot}$ and the photospheric rotational velocity, $V_{\rm phot}$. For the satellite components of the Si IV resonance lines, the maximum ratio, $V_{\rm rot}/V_{\rm phot}$, varies from 19 for the first, to 1 for the fifth component (figure 5).

5.3. Rotation in Photosphere vs. Rotation of Density Regions

As one can see in figures 4 and 5, there is a good correlation between the rotational velocities of the density regions and the photosphere. In both cases (Be and Oe stars) for rotational velocity of the photosphere, $V_{\rm phot} > 200$ km s^{-1}, the rotation of the photosphere correlates with the rotation of the density regions ($V_{\rm rot} \approx$ const. $\times\, V_{\rm phot}$). On the other hand, for $V_{\rm phot} < 200$ km s^{-1}, the ratio $V_{\rm rot}/V_{\rm phot}$ decreases with the

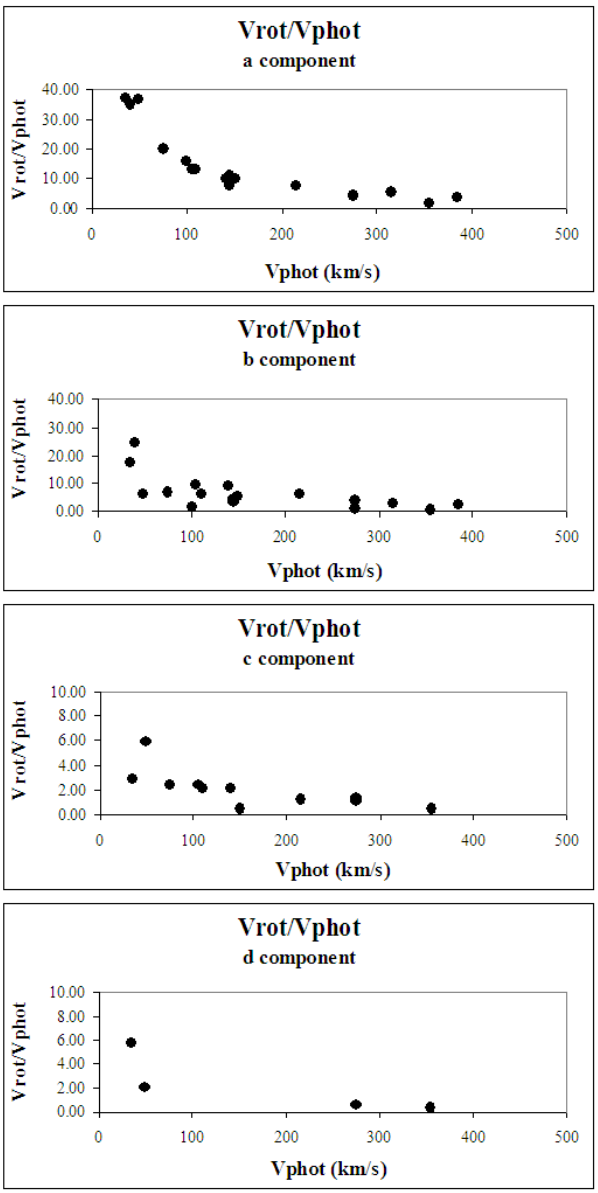

Fig. 4. Ratio $V_{\rm rot}/V_{\rm phot}$ of the four SACs as a function of the photospheric rotational velocity ($V_{\rm phot}$) for all of the studied Oe stars.

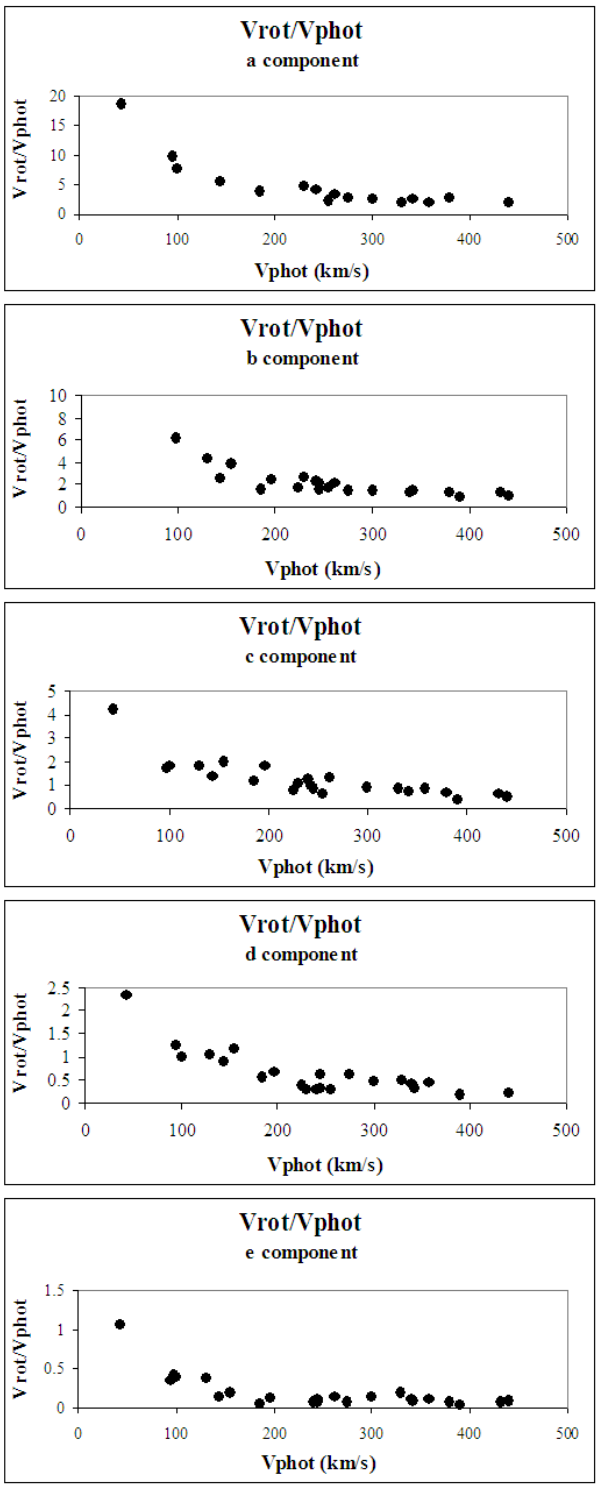

Fig. 5. Ratio $V_{\rm rot}/V_{\rm phot}$ of the five SACs as a function of the photospheric rotational velocity ($V_{\rm phot}$) for all of the studied Be stars.

rotation in the photosphere. This can be explained by the inclination effect and the fact that the density regions are extensive around the star, i.e., for a high inclination angle the projected photospheric rotational velocity is small, but in a density region (that lies extensively around the star), one can detect faster rotation.

6. Conclusions

Here we present a new model for fitting the complex UV lines of Be and Oe stars, where we take into account the possibility that the random motion of ions can significantly contribute to the line widths. The proposed model can be applied to the spectral photospherical lines as well as the UV lines originating in the post-coronal regions. Concerning our work, we can make the following conclusions:

(i) The proposed model can accurately reproduce the complex UV lines of Be and Oe stars.

(ii) Using the proposed model one can very well separate the contribution of the rotational and radial velocities in the density region by fitting the complex line profiles.

(iii) The proposed model provides an opportunity to investigate the physical parameters of the regions creating the UV complex line profiles.

(iv) The proposed model allows us to use the photospheric lines, in order to determine the photospheric rotation.

At the end, let us point out that in spite of the fact that today there exists a number of models that are able to reproduce the spectra from stellar atmospheres, there is a problem to find an appropriate model that can fit the complex UV line profiles that are created not only in the photosphere, but also in the density regions. On the other hand, the proposed model is able to provide information about the physical parameters of density regions as well as the rotation of the photosphere. We hope that the proposed model will be useful first of all to allow a first impression about the physics of density layers.

We would like to thank Professor Ryuko Hirata for his very useful suggestions. This research project is progressing at the University of Athens, Department of Astrophysics - Astronomy and Mechanics, under the financial support of the Special Account for Research Grants, which we thank very much. The project is co-financed within Op. Education by the ESF (European Social Fund) and National Resources, under the "Herakleitos" project. This work also was supported by Ministry of Science of Serbia, through the following projects: *Influence of collisional processes on astrophysical plasma line shapes* - P146001 and *Astrophysical spectroscopy of extragalactic objects* - P146002.

Appendix. Including the Random Motion in the Calculation of L — The Gauss-Rotation model (GR model)

We consider a spherical shell and a point A_i in its equator. If the laboratory wavelength of a spectral line that arises from A_i is $\lambda_{\rm lab}$, the observed wavelength is: $\lambda_0 = \lambda_{\rm lab} \pm \Delta\lambda_{\rm rad}$. If the spherical density region rotates, we observe a displacement $\Delta\lambda_{\rm rot}$ and the new wavelength of the center of the line is $\lambda_i = \lambda_0 \pm \Delta\lambda_{\rm rot}$, where $\Delta\lambda_{\rm rot} = \lambda_0 z \sin\varphi$, $z = \dfrac{V_{\rm rot}}{c}$, $V_{\rm rot}$ is the rotational velocity of point A_i.

This means that $\lambda_i = \lambda_0 \pm \lambda_0 z \sin\varphi = \lambda_0 (1 \pm z \sin\varphi)$ and if $-\dfrac{\pi}{2} < \varphi < \dfrac{\pi}{2}$, then $\lambda_i = \lambda_0 (1 - z \sin\varphi)$.

If we consider that the spectral line profile is a Gaussian distribution, $I(\lambda) = \dfrac{1}{\sqrt{2\pi}\sigma} e^{-\left[\frac{\lambda-\kappa}{\sigma\sqrt{2}}\right]^2}$, where κ is the mean value of the distribution and in the case of the line profile it indicates the center of the spectral line that arises from A_i. This means that

$$I(\lambda) = \frac{1}{\sigma\sqrt{2\pi}} e^{-\left[\frac{\lambda-\lambda_0(1-z\sin\varphi)}{\sigma\sqrt{2}}\right]^2} = \frac{1}{\sigma\sqrt{2\pi}} e^{-\frac{[\lambda-\lambda_0(1-z\sin\varphi)]^2}{2\sigma^2}}. \tag{A1}$$

The distribution function for all of the semi-equator is

$$I_1(\lambda) = \int_{-\frac{\pi}{2}}^{\frac{\pi}{2}} \frac{1}{\sqrt{2\pi}\sigma} e^{-\frac{[\lambda-\lambda_0(1-z\sin\varphi)]^2}{2\sigma^2}} \cos\varphi d\varphi. \tag{A2}$$

If $\sin\varphi = x$, then $dx = \cos\varphi d\varphi$, $-1 \le x \le 1$, and equation (A2) takes the form

$$I_1(\lambda) = \int_{-1}^{1} \frac{1}{\sigma\sqrt{2\pi}} e^{-\frac{[\lambda-\lambda_0(1-zx)]^2}{2\sigma^2}} dx. \tag{A3}$$

If we set $u = \dfrac{\lambda - \lambda_0(1-zx)}{\sqrt{2}\sigma}$, we have

$$I_1(\lambda) = \frac{1}{\lambda_0 z\sqrt{\pi}} \int_{\frac{\lambda-\lambda_0(1+z)}{\sigma\sqrt{2}}}^{\frac{\lambda-\lambda_0(1-z)}{\sigma\sqrt{2}}} e^{-u^2} du. \tag{A4}$$

We consider the function $\operatorname{erf}(x) = \dfrac{2}{\pi}\displaystyle\int_0^x e^{-u^2} du$. It is a known function that describes the Gaussian error distribution.

If we take into account this function, $I_1(\lambda)$ takes the form

$$I_1(\lambda) = \frac{1}{\lambda_0 z\sqrt{\pi}} \left[\int_0^{\frac{\lambda-\lambda_0(1-z)}{\sigma\sqrt{2}}} e^{-u^2} du - \int_0^{\frac{\lambda-\lambda_0(1+z)}{\sigma\sqrt{2}}} e^{-u^2} du \right], \tag{A5}$$

$$I_1(\lambda) = \frac{1}{\lambda_0 z\sqrt{\pi}} \left\{ \frac{\pi}{2} \operatorname{erf}\left[\frac{\lambda-\lambda_0(1-z)}{\sigma\sqrt{2}}\right] - \frac{\pi}{2} \operatorname{erf}\left[\frac{\lambda-\lambda_0(1+z)}{\sigma\sqrt{2}}\right] \right\}. \tag{A6}$$

Thus, we finally have

$$I_1(\lambda) = \frac{\sqrt{\pi}}{2\lambda_0 z} \left[\operatorname{erf}\left(\frac{\lambda-\lambda_0(1-z)}{\sigma\sqrt{2}}\right) - \operatorname{erf}\left(\frac{\lambda-\lambda_0(1+z)}{\sigma\sqrt{2}}\right) \right], \tag{A7}$$

and the distribution function from the semi-spherical region is

$$I_{\rm final}(\lambda) = \frac{\sqrt{\pi}}{2\lambda_0 z} \int_{-\frac{\pi}{2}}^{\frac{\pi}{2}} \left[\operatorname{erf}\left(\frac{\lambda-\lambda_0}{\sigma\sqrt{2}} + \frac{\lambda_0 z}{\sigma\sqrt{2}}\cos\theta\right) - \operatorname{erf}\left(\frac{\lambda-\lambda_0}{\sigma\sqrt{2}} - \frac{\lambda_0 z}{\sigma\sqrt{2}}\cos\theta\right) \right] \cos\theta d\theta, \tag{A8}$$

(Method Simpson).

In equation (A8), from λ_0 we can calculate the value of the radial velocity ($V_{\rm rad}$); from z we calculate the rotational velocity ($V_{\rm rot}$), and from σ we calculate the random velocity ($V_{\rm rand}$).

This distribution function, $I_{\rm final}(\lambda)$, has the same form as the distribution function of the absorption coefficient, L, and may replace it in the line functions $e^{-L\xi}$ or $S_{\lambda e}\left(1 - e^{-L_{ej}\xi_{ej}}\right)$, in the case when the line broadening is an effect of both the rotational velocity of the density region as well as the random velocities of the ions. This means that we now have a new distribution function to fit each satellite component of a complex line profile that represents DACs or SACs. We name this function the Gauss-Rotation distribution function (GR distribution function).

References

Antoniou, A., Danezis, E., Lyratzi, E., Nikolaidis, D., Popović, L. Č., Dimitrijević, M. S., & Theodossiou, E. 2006, in Proc. 23rd Summer School and International Symposium on the Physics of Ionized Gases, ed N. S. Simonović, B. P. Marinković, & L. Hadžievski (Melville, NY: AIP)

Bates, B., & Halliwell, D. R. 1986, MNRAS, 223, 673

Chauville, J., Zorec, J., Ballereau, D., Morrell, N., Cidale, L., & Garcia, A. 2001, A&A, 378, 861

Cranmer, S. R., & Owocki, S. P. 1996, ApJ, 462, 469

Cranmer, S. R., Smith, M. A., & Robinson, R. D. 2000, ApJ, 537, 433

Danezis, E. 1983, PhD Thesis, University of Athens

Danezis, E. 1987, in IAU Colloq. 92, Physics of Be Stars, ed A. Slettebak & T. P. Snow (Cambridge, UK: Cambridge University Press), 445

Danezis, E., et al. 2003, Ap&SS, 284, 1119

Danezis, E., Lyratzi, E., Nikolaidis, D., Antoniou, A., Popović, L. Č., & Dimitrijević, M. S. 2006, in Proc. 23rd Summer School and International Symposium on the Physics of Ionized Gases, ed. N. S. Simonović, B. P. Marinković, & L. Hadžievski (Melville, NY: AIP)

Danezis, E., Nikolaidis, D., Lyratzi, E., Popović, L. Č., Dimitrijević, M. S., Theodossiou, E., & Antoniou, A. 2005, Mem. Soc. Astron. Ital., 7, 107

Fullerton, A. W., Massa, D. L., Prinja, R. K., Owocki, S. P., & Cranmer, S. R. 1997, A&A, 327, 699

Grady, C. A., Sonneborn, G., Wu, C.-C., & Henrichs, H. F. 1987, ApJS, 65, 673

Henrichs, H. F. 1984, in ESA SSSP-218, Proc. 4th European IUE Conf., ed E. Rolfe & B. Battrick (Noordwijk: ESA), 43

Kaper, L., et al. 1997, A&A, 327, 281

Kaper, L., Henrichs, H. F., Nichols, J. S., Snoek L. C., Volten, H., & Zwarthoed G. A. A. 1996, A&AS, 116, 257

Kaper, L., Henrichs, H. F., Nichols, J. S., & Telting, J. H. 1999, A&A, 344, 231

Lamers, H. J. G. L. M., Snow, T. P., de Jager, C., & Langerwerf, A. 1988, ApJ, 325, 342

Lyratzi, E. & Danezis, E. 2004, in AIP Conf. Proc., 740, 458

Lyratzi, E., Danezis, E., Nikolaidis, D., Antoniou, A., Popović, L. Č., & Dimitrijević, M. S., & Theodossiou, E. 2006, in Proc. 23rd Summer School and International Symposium on the Physics of Ionized Gases, ed. N. S. Simonović, B. P. Marinković, & L. Hadžievski (Melville, NY: AIP)

Lyratzi, E., Danezis, E., Popović, L. Č., & Dimitrijević, M. S., Nikolaidis, D., & Antoniou, A. 2007, PASJ, 59, 357

Markova, N. 2000, A&AS, 144, 391

Mullan, D. J. 1984a, ApJ, 283, 303

Mullan, D. J. 1984b, ApJ, 284, 769

Mullan, D. J. 1986, A&A, 165, 157

Nikolaidis, D., Danezis, E., Lyratzi, E., Popović, L. Č., Antoniou, A., Dimitrijević, M. S., & Theodossiou, E. 2006, in Proc. 23rd Summer School and International Symposium on the Physics of Ionized Gases, ed. N. S. Simonović, B. P. Marinković, & L. Hadžievski (Melville, NY: AIP)

Prinja, R. K., & Howarth, I. D. 1988, MNRAS, 233, 123

Rivinius, Th. et al. 1997, A&A, 318, 819

Underhill, A. B. 1975, ApJ, 199, 691

Underhill, A. B., & Fahey, R. P. 1984, ApJ, 280, 712

Waldron, W. L., Klein, L., & Altner B. 1992, ASP Conf. Series, 22, 181

Waldron, W. L., Klein, L., & Altner B. 1994, ApJ, 426, 725

Wilson, R. E. 1963, General Catalogue of Stellar Radial Velocities (Washington: Carnegie Institution of Washington), 601